rate, fluorine injection. Long prepressurization times (23 sec) were required to reach 100 psig, and this long, continuous, high-velocity fluorine injection probably created a hole in the LH_2 that reached from the injector to the ullage along the tank centerline. The vapor in this ullage extension was heated by injection in the same way that US mode injection heats the ullage, which gave a high initial pressurization efficiency that is comparable to that of the US mode. Further, at this high tank pressure, the LH_2 outflow rate was quite high, so that the drain from an ullage fraction of 44–78% (shown as the straight solid line) took place in only 6.6 sec. This short time gives little opportunity for heat transfer and could explain the fact that efficiency remained uniform and high. Again, with large ullage volume (and empty tank), all of the injection modes tend to an efficiency value of about 50% of the ullage heating prediction.

Conclusions

Fluorine injection into a liquid hydrogen tank provides efficient tank pressurization by ullage heating, rather than by vaporization of hydrogen. Manual control of the pressure during prepressurization and expulsion has been demonstrated, and the extension to an automatic tank-pressure control system appears straightforward.

The ullage-simple injector mode demonstrated an efficiency of 40–80% for tank prepressurization and propellant expulsion. The submerged aspirated injector did not operate satisfactorily: it could not pump (by aspiration) sufficient hydrogen for vaporization and injector cooling. The injector always operated extremely oxidizer(fluorine)-rich and very hot, which resulted in severe damage to the injector as the tank emptied. The submerged-simple injection mode has pressurization efficiency of about 2% operating into a full tank, because of large heat losses to the liquid. The efficiency improves to as much as 40% as the tank empties. Work is in progress to develop models that include provisions for heat-transfer modes, to permit more confident extrapolation from the existing test data to arbitrary tank sizes and liquid levels.

References

[1] Kenny, R. J. and Friedman, P. A., "Chemical Pressurization of Hypergolic Liquid Propellants," *Journal Spacecraft and Rockets*, Vol. 2, No. 5, Oct. 1965, p. 746–753.

[2] Van Der Lingen, "A Jet Pump Design Theory," *Transactions of the ASME Series D: Journal of Basic Engineering*, Dec. 1960, pp. 947–960.

NOVEMBER 1969 J. SPACECRAFT VOL. 6, NO. 11

Measurement of Solid Rocket Motor Thermally Induced Radial Bond Stresses

W. H. MILLER*

Rocketdyne, A Division of North American Rockwell Corporation, McGregor, Texas

Through-the-case, semiconductor load transducers† were utilized in a prototype solid propellant rocket motor to monitor thermally induced, case-to-liner normal bond stresses. Grain cross-sectional design was cross dogbones; length-to-diameter ratio was 5.5. Six thermal cycles were made between 160° and −65°F. Characteristics of the transducers are discussed briefly, and data for nine longitudinal and circumferential stations are presented. Characteristics of the stress increase/decay with conditioning temperature reduction/rise are described along with the reductions in magnitudes which were measured with each ensuing temperature cycle. Bond stresses predicted analytically are compared with measured data.

Introduction

THE analyst is required to predict stress-strain magnitudes and distributions induced in nonlinear viscoelastic materials when designing case-bonded, solid propellant rocket motor grains. The stress induced in the liner and propellant at the case bond line is of prime interest. Numerical techniques currently used by industry for stress-strain predictions, although most useful, require numerous limiting approximations. These are involved in the selection of the mathematical model, approximating analytically the properties of viscoelastic materials, and the analytical duplication of the load-inducing, motor environmental conditions. Ultimate success of a grain design analysis is measured by the ability of production grains to endure service environments without failure. Thus, it is desirable to measure stress-strain states in full-scale motors and by so doing to obtain guidance and assurance with respect to the assumptions necessary to permit confident analytical assessments of the structural capability of future grain designs.

As one step toward accomplishing this objective, Rocketdyne developed a semiconductor load cell that permits the analyst to experimentally determine normal stresses at the bond line between two rheologically different materials. This instrumentation was first used in tests of 4-in.-diam test vehicles containing case-bonded propellant grains with cylindrical ports.[1] Ensuing tests were made with a prototype structural test motor more representative in size and configuration of a full-scale missile propulsion system.[2] Results from the latter are presented herein. Loads were induced thermally by temperature cycling under development-program-type test conditions.

Presented as Paper 68-510 at the ICRPG/AIAA 3rd Solid Propulsion Conference, Atlantic City, N.J., June 4–6, 1968; submitted October 21, 1968; revision received August 4, 1969. This work was supported by Rocketdyne's Independent Research and Development Program, 1966–1967. Numerous members of the technical staff at Rocketdyne contributed significantly to this program. The author is especially thankful to J. D. Burton for his assistance with data evaluation.

* Member of Technical Staff, Solid Rocket Division. Member AIAA.

† Patent 3,389,598.

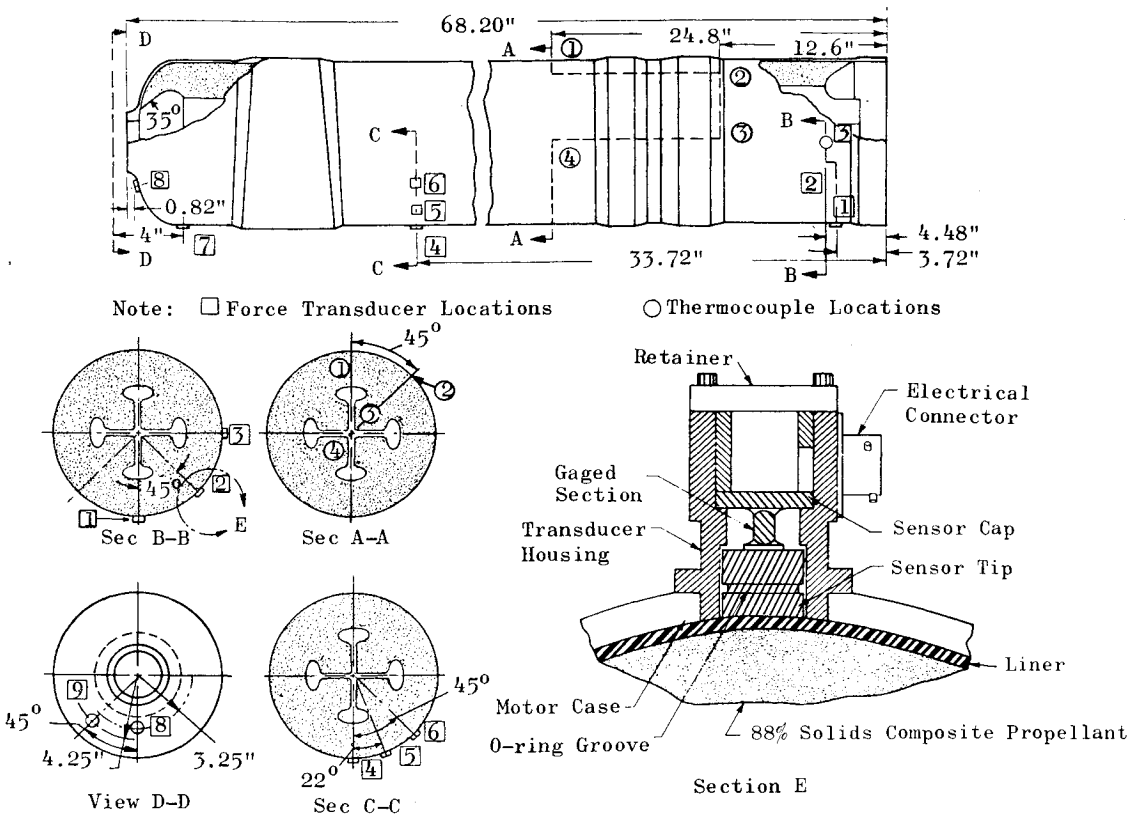

Fig. 1 Instrumented motor and bond stress sensor assembly details.

The instrumented motor was subjected to six temperature cycles between 160° and −65°F. Cycles consisted of both shock-type, a single-temperature step from 160° to −65°F, and multistepped cooling. In the latter type cycle, thermal equilibrium was approximately achieved at each of the intermediate temperature steps. Data were obtained automatically at 15-min intervals.

The primary objective of this program was to determine thermally induced stresses with the motor in a state of thermal equilibrium at various temperatures. However, qualitative thermal transient data were obtained and are likewise reviewed. Numerically predicted stresses are compared for selected equilibrium conditions. The analytical technique used is common to the industry and utilizes a finite element representation of the structure.[3]

Test Vehicle

A crossed-dogbone grain configuration, Fig. 1, was selected for the full-scale test vehicle. Grain-to-case termination geometries were based on Rocketdyne-sponsored, photoelastic studies.[4] Nominal motor case and liner thicknesses were 0.085 and 0.05 in., respectively. Inside case diameter was 12.25 in.; grain length-to-diameter ratio was 5.5.

Instrumentation

Considerable progress has been made by the industry in developing instrumentation for experimental determination of stresses and strains in solid propellant grains. As exemplified in a recent comprehensive literature survey,[5] many design types have been and are being developed for various applications. The sensor discussed herein was developed[1] for measuring normal stresses at bond lines between a motor case and propellant or liner. It incorporates semiconductor strain gages mounted on the walls of a hollow column. This piston-type, through-the-case transducer is comprised of the major components shown in the assembly cross-section in view E of Fig. 1. Notable features of the design include: 1) a gaged section threaded on one end, permitting the sensor tip to be held in place during case lining and propellant casting by a higher strength nongaged section; 2) housing and transducer metallic components are matched to reduce differences in the thermal expansion between components; 3) a hollow gaged section makes sensor amenable to in-place calibration; 4) a sensor tip that can be removed from gaged section, permitting tip size selection with each application and reuse of gaged section; 5) semiconductor strain gages whose resistance-temperature characteristics can be selected to provide a thermally compensative transducer within the electrical circuit of the gage.

The design permits installation of the gaged sections either before or after propellant casting and curing. If the motor is to be fired, the gaged sections can be removed and pressure plugs installed. General calibration and load characteristics of the gaged sections used in this test program are 1) minimum over-range capability: linearity (% full-scale best fit line) = ±0.25% and hysteresis (% f.s.) = ±0.25%; 2) balance temperature stability (% f.s.) = ±1%/100°F; 3) temperature stability (% f.s.) = ±0.25%/100°F; 4) maximum output voltage = 400 mv; 5) load range = 0 to 150 psi; 6) maximum extension under loads of this test = 130 μin.; 7) diameter of rigid probe tip = 0.5 in.

The sensors with auxiliary electrical cabling were, as units, not totally temperature compensative. Thus, each transducer unit was calibrated over the expected temperature and load ranges. These calibration data established zero shifts and load sensitivity variations with temperature. Calibration loads were tensile and applied by suspending weights from adaptors that in turn were attached (threaded connections) to the gaged sections. These bench-type tests were conducted within the conditioning chamber in which the motor was thermally cycled and with the respective electrical leads and through the automatic data retrieval system. This practice was exercised to reduce instrumentation uncertainties. Calibration tests were run before cycling and during the test and were checked following test completion (Fig. 2). The repeatability was good between these data as maximum variations were less than 5%. Calibration data were curve fit for computerized reduction of motor test data.

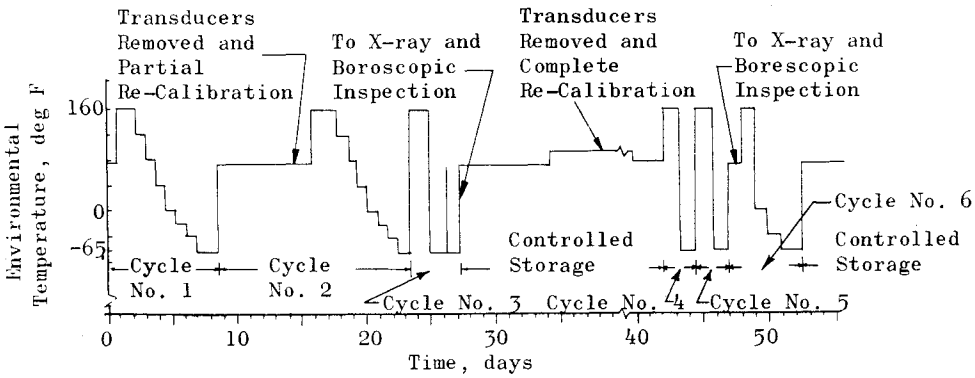

Fig. 2 Sequence and type of temperature cycles.

Another variable is introduced with the use of a piston-type transducer. This is the influence on the stress field in the immediate vicinity of the sensor tip. A structural evaluation of the hollow section indicated a maximum extension of 130 μin. could be encountered with the loading in this particular application. The exact extent to which the displacement could influence the local stress field was not known at the time of these tests. However, a cursory, numerical evaluation was made to get an approximate assessment. Finite-element models were used, and various combinations were assumed for propellant, liner, and transducer material properties. This parametric evaluation indicated this maximum extension could possibly introduce a 3% error in the experimental data for a combination of properties believed characteristic of the system reported herein. Thus, with calibration variations and possible compliance variations, results of this program were expected to indicate stresses well within an accuracy of $\pm 10\%$.

Assembly details of the transducer are shown in Fig. 1 along with the locations of the nine load transducers and the grain and case thermocouples. Longitudinal distribution of the transducers was divided equally between the forward, central, and aft regions of the grain. The transducers were placed to provide circumferential stress distribution data within each region. Load transducer data were supplemented with data from thermocouples mounted on the grain inner bore and on the case exterior.

Thermal Cycling Program

A complete thermal history of this prototype motor is summarized graphically in Fig. 2. The motor was subjected to six temperature cycles, the upper and lower extremes of which were 160° and −65°F (±5°F), respectively. Temperature steps of various magnitudes were used for cooling the motor after it was conditioned at 160°F. It was step cooled in 20- or 40-deg steps to the lower extreme of −65°F during cycles 1, 2, and 6 and was shock-cooled from 160°F directly to −65°F during cycles 3, 4, and 5. It was conditioned for 18 hours at each temperature step in the step-cooling cycles. This permitted the grain to achieve thermal equilibrium to within 5°F at each step. This conditioning time was increased to a minimum of 24 hr at the thermal extremities of the cycles, i.e., 160° and −65°F. Conditioning periods were based on pretest heat transfer analyses that were, in turn, confirmed by thermocouple data.

Experimental Results

Experimentally measured liner-to-case bond stresses were supplemented with grain inner-bore and external case temperatures. Examples of typical data in the form of time histories for one of the single and multistep temperature cycles are presented in Figs. 3 and 4, respectively. Figure 3 includes the output from thermocouples measuring the temperature of the conditioning box, the motor case, and the grain inner bore. Conditioning time necessary to reach the maximum bond stress for the shock cycle was approximately 28 hr. As expected, this varied along the length of the motor. Data have been corrected to account for thermally induced zero shifts. However, data obtained during the initial hours of each temperature step were considered only qualitatively because a finite time period is required for the transducer and gaged section to achieve thermal equilibrium. After the motor achieved near thermal equilibrium at each temperature step, the transducer-gaged element temperature was likewise

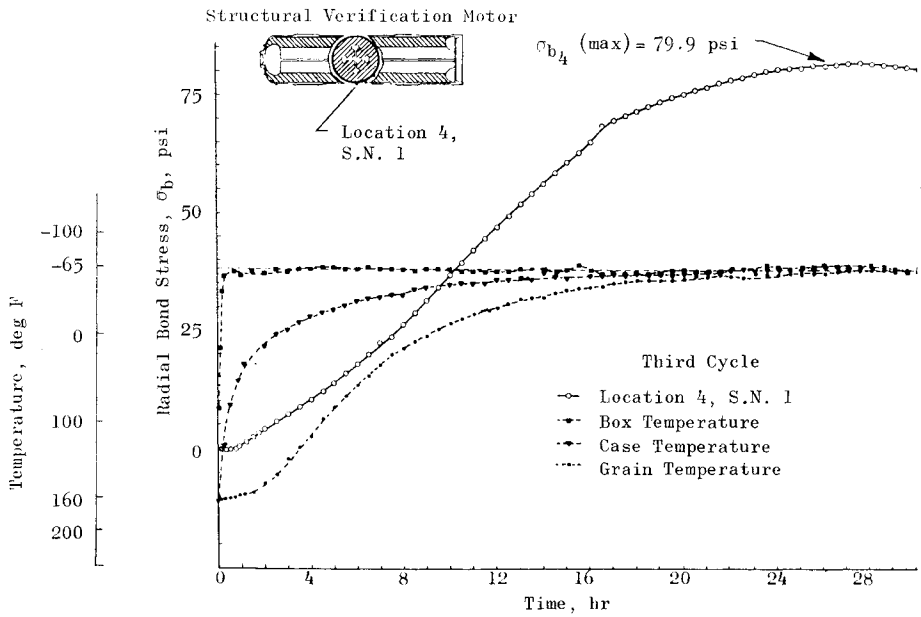

Fig. 3 Typical data variation for shock thermal loading.

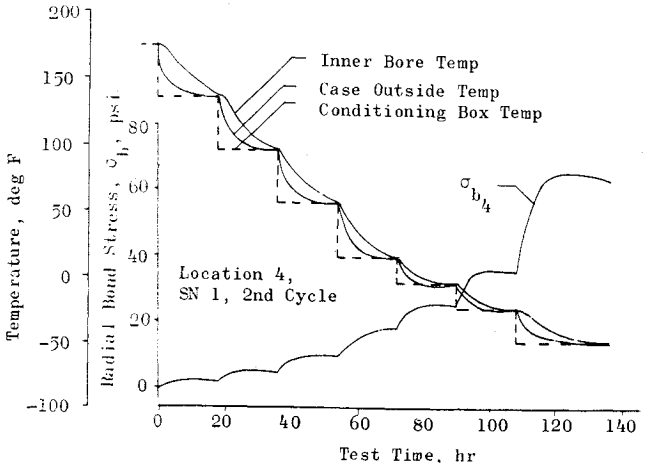

Fig. 4 Typical multistepped cycle data.

assumed in equilibrium, and results could be treated quantitatively. Raw data of a similar nature were presented in Ref. 2.

Figure 4 depicts typical transducer output during a temperature cycle in which the motor was cooled in 40- and 20-deg decrements. Note the progressive increase in the equilibrium stresses as the motor is step-cooled to lower temperatures. This characteristic is associated with the nonlinear, viscoelastic nature of the propellant. A summary of these equilibrium bond stress data along with that from the other five temperature cycles is presented in Fig. 5 for the three transducers located at the motor longitudinal center. Similar summaries for all nine transducers were presented in Ref. 2. Data points shown therein are averages of values taken over a time span of 1 hr (four measurements) after the motor had achieved thermal equilibrium at each step. Thus, referring again to Fig. 4, at each temperature step at which the motor was conditioned, a value of bond stress was so determined and plotted as a function of equilibrium temperature. This was done for each transducer. The 1-hr span and the four consecutive readings were selected to produce the maximum average equilibrium stress at each temperature. Thus, these average stresses do not include significant relaxation. It was not the intent of the tests to obtain relaxation data per se.

As the gaged sections of the transducers are interchangeable, an additional precaution was taken to check out instrumentation in this initial full-scale prototype motor test program. Several load sensors were interchanged between cycles to check out transducer-to-transducer repeatability. For this reason, transducer serial number (S/N) and cycle number are identified in the summary plots. Over-all evaluation of test data revealed the transducer design to be readily amenable to gaged section interchange with no degradation in data.

One of the most significant general characteristics of these experimentally determined, thermal equilibrium stresses was the reduction in magnitude with each ensuing temperature cycle. This is noted by comparing the curves fared through the equilibrium data points (Fig. 5) obtained from stepped cycles 1, 2, and 6. Hilzinger,[6] in describing this phenomena, refers to it as the Mullin's effect; it is attributed to dewetting

Sym	Cycle No.	Loading	Transducer Serial No. Loc 4	Loc 5	Loc 6
○	1	Stepped	1	12	4
◇	2	Stepped	1	12	4
○	3	Shocked	1	12	4
△	4	Shocked	6	12	1
□	5	Shocked	6	12	1
▽	6	Stepped	6	12	1
Analytically Predicted Stress Values	●	—	Shocked--Assuming Highly Rigid Motor Case		
	◥	—	Shocked--Assuming Flexible Motor Case		

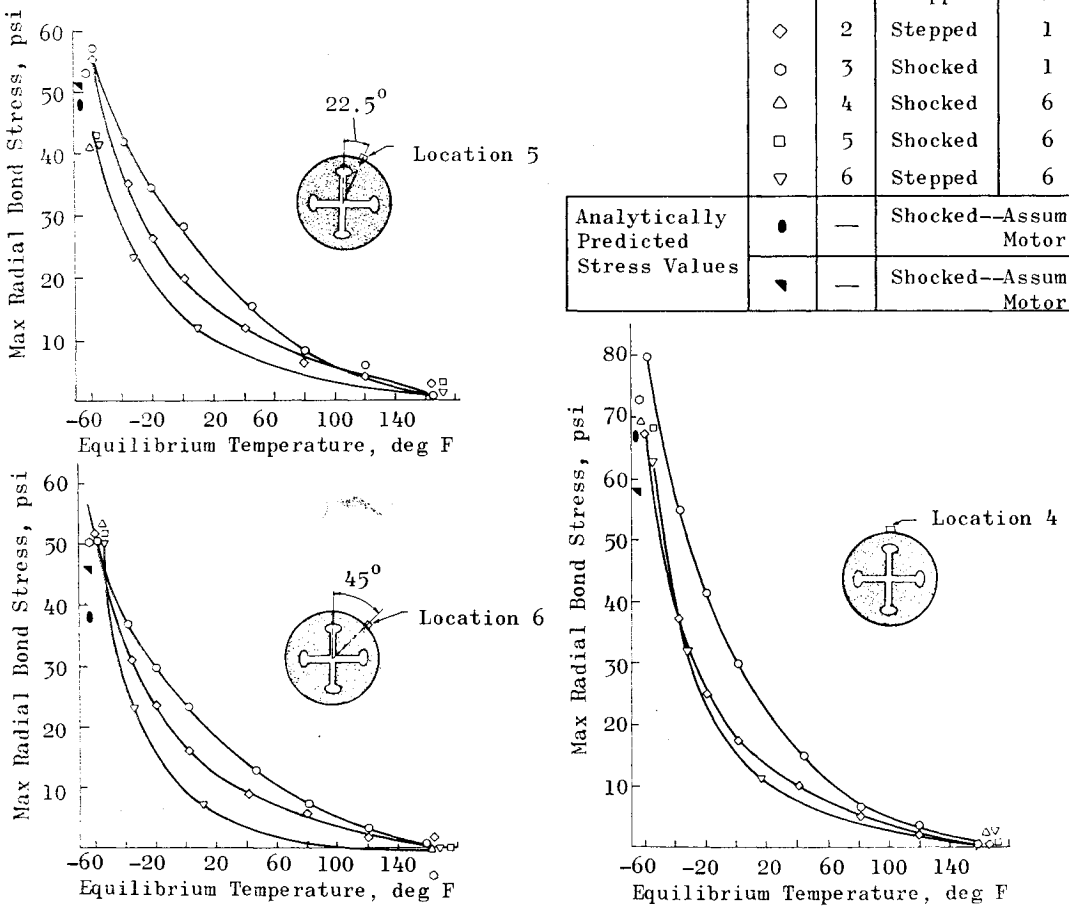

Fig. 5 Typical maximum radial bond stresses under thermal equilibrium conditions.

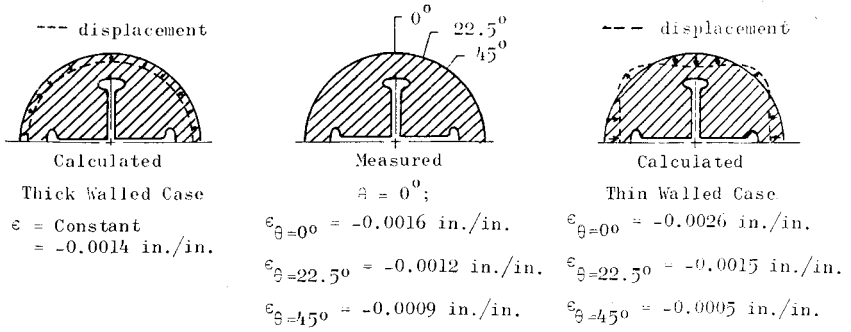

Fig. 6 Measured and calculated average strain distributions.

between binder and oxidizer particles. Using JANAF (Joint Army-Navy Air Force) uniaxial tensile specimens subjected to repeated nondestructive loading cycles, Hilzinger's tests also revealed, as do these motor data, that the magnitude of the decrement decreases with increasing numbers of cycles.

In interpreting the data in Fig. 5, one should remember that the lower conditioning temperature, −65°F, has specified ±5°F variational limits. Upon final data reduction, variations were found to be $^{+8}_{-3}$ deg. These are reflected in the plotted data.

A high-speed computer program using finite element techniques[3] was utilized in the numerical prediction of bond stresses. Both flexible (thin wall) and rigid (thick wall) motor case-type analytical models were considered as the thick sections of the case were believed to be close enough to influence case rigidity at the motor longitudinal center. Strain gages were placed on the case midway through the test program in an attempt to substantiate this opinion. Measured and calculated average strain distributions are compared in Fig. 6.

Comparison of the measured strains with the calculated values indicates loading in the region of the grain shown is probably closer to that of a flexible case (i.e., propellant shrinkage does influence case deflection). However, neither could be considered totally correct along the full length of the motor because of case geometry (Fig. 1). Thus, analytical predictions for both loading conditions were considered in the correlation study.

Analytical Correlation

Structural integrity of the prototype grain design was analytically assessed for the extreme thermal loading condition of −65°F. This analysis, utilizing finite-element techniques, assumes a linearly elastic numerical solution to the thermally induced stress and strain fields that exist in the solid propellant grain. A high-speed computer program,[3] developed by Rohm and Haas, was used in these calculations. Computer inputs included grain geometry; material properties such as modulus, Poisson's ratio, and thermal coefficients of expansion; incremental change in temperature. The stress-strain free thermal condition was assumed to be 160°F. This was selected for correlation as it corresponded with the upper thermal extreme of the temperature cycles. Analyses were made for only the lowest equilibrium conditioning temperature, −65°F.

A propellant strain rate of 1.85×10^{-5} in./in./min and an equilibrium soak temperature of −65°F were used in selecting moduli from mechanical property spectrums: 2000 psi for propellant, 120 psi for liner, and 30×10^6 psi for the case. Propellant modulus was determined from a secant modulus spectrum generated from JANAF uniaxial tab-ended specimen tests. Loading conditions within the motor are biaxial and triaxial and not uniaxial. However, multi-axial characterization data were not available for these analyses. The lack of such data is a frequent problem encountered by the analyst as mechanical property characterization is much more expensive and time consuming for multiaxial loadings. Thus, as in this study, uniaxial mechanical properties are frequently substituted and more conservative design margins of safety are required. The strain rate was based on an average strain calculated across the grain web at the dogbone slots. The average strain was 0.03 in./in.; a 27-hr conditioning time was required to induce this strain. Transient stress data indicated the major portion of the thermal load was induced during this time interval (Fig. 3). A Poisson's ratio of 0.499 was assumed for both liner and propellant.

The analyzed regions of the grain were simulated geometrically by finite-element grid models illustrated in Ref. 2. These were 1) a plane strain model, the loading condition assumed to exist at the longitudinal center of the grain and 2) axisymmetric models simulating the grain forward and aft-end contours. The web fraction assumed for the axisymmetric models was such that the maximum bond stress predicted for a cylindrically perforated grain of this web fraction would correspond to the maximum value predicted in the rigid case, plane strain analysis of the crossed-dogbone configuration (Fig. 7).

Figure 8 compares the distribution of predicted and measured stresses normal to the case-liner bond line for the thermal equilibrium condition of −65°F. These data are for positions along the grain along the grain adjacent the dogbones and in the axisymmetric region of the motor forward end. The analytically predicted values at the longitudinal center of the grain were slightly low, whereas the value predicted at the very forward tip of the grain was high. Figure 7 compares the analytically predicted circumferential stress distributions at the longitudinal center of the grain with experimentally measured data.

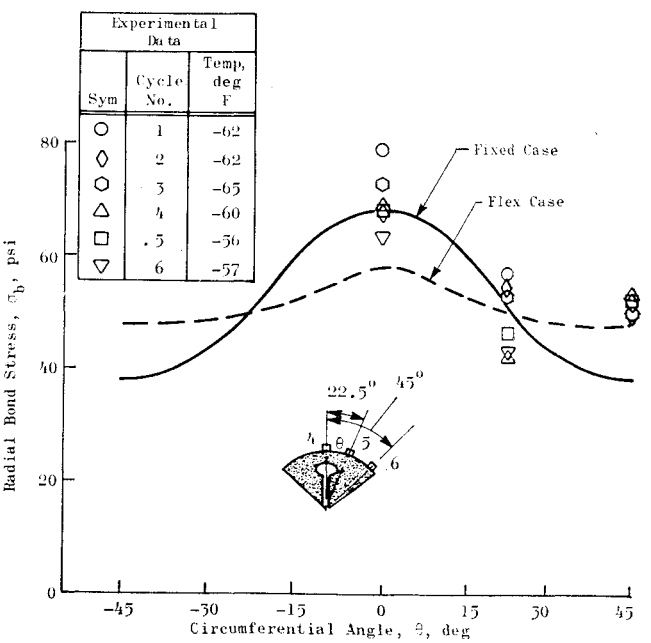

Fig. 7 Motor longitudinal midsection radial bond stress distributions.

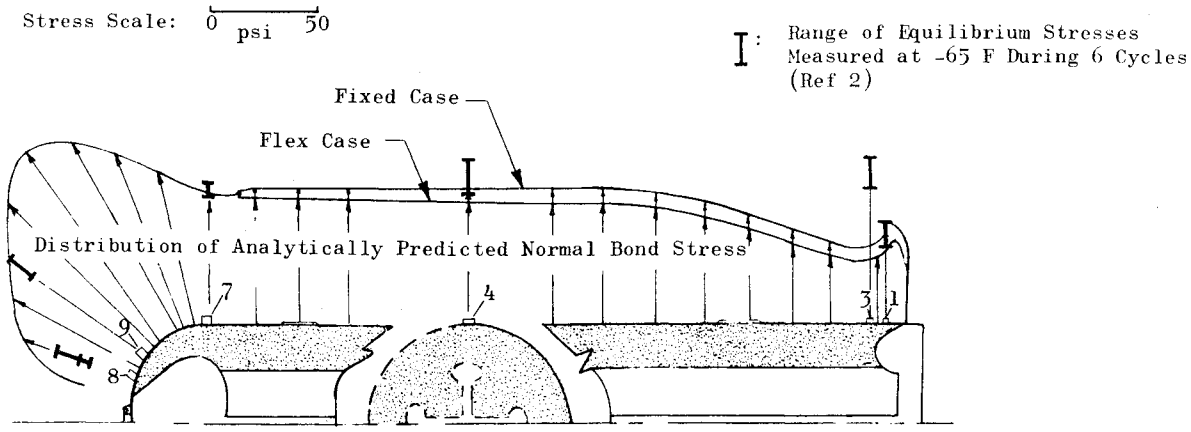

Fig. 8 Correlation of stress distributions normal to caseliner bond line.

In general, measured stresses at T = −65°F compared favorably with numerically predicted values. Sources for disagreement are believed to stem primarily from 1) making a 2-D numerical analyses of a 3-D problem using one-dimensional material properties, 2) making linearly elastic analyses of a nonlinear viscoelastic problem, and 3) instrumentation uncertainties. Instrumentation anomalies that have not been completely resolved center primarily around transducer-propellant compliance. These were reviewed previously.

Conclusions

This program proved through-the-case bond stress transducer instrumentation to be amenable for use on full-scale solid propellant motors under treatment typical of a development-type program. Transducers were shown to be valuable tools whereby data could be obtained to define the mechanical response of propellant grains to thermal loadings. The potential of this instrumentation was not totally used in these tests as only the data at equilibrium temperatures were considered quantitatively. The program provided cycle end point numerical and experimental correlations. Only end point analyses are made during the investigation of the structural integrity of a given grain design because of the complex 3-D geometries typical of solid propellant grains; the nonlinear, viscoelastic characteristics of propellant; current state-of-the-art analytical techniques. These test results and the analytical correlations have been used advantageously in ensuing design analyses.

The bond stress transducer used in this program is only the first in Rocketdyne's continuing series of improvements in instrumentation for monitoring response of solid propellant rocket motor grains. Current and future plans encompass continued studies on analogue laboratory-type motors (cylindrical ports) and full-scale research and development-type grains that fully comply with both structural and ballistic requirements.

References

[1] Cousins, T. E., "A Transducer for Measuring Radial Bond Stresses in Solid Propellant Rocket Motors," *Insulation and Case Bonding Symposium*, CPIA Publication No. 159, Sept. 1967, Chemical Propulsion Information Agency, p. 195.

[2] Miller, W. H., "Experimentally Measured Radial Bond Stresses in a Full-Scale Motor," AIAA Paper 68–510, Atlantic City, N.J., 1968.

[3] Becker E. B. and Brisbane, J. J., "Application of the Finite Element Method to Stress Analysis of Solid Propellant Rocket Grains," Rept. S–76, Jan. 1966, Rohm and Haas.

[4] Parks, V. T. and Durelli, A. J., "Stress Distributions at Variously Shaped Corners in Plates, Bonded on Two Long Edges, and Subjected to Restrained Shrinkage," *Proceedings of 5th Meeting Behavior Working Group*, Vol. I, ICRPG, CPIA Publication No. 119, Nov. 1966, Interagency Chemical Rocket Propulsion Group and Chemical Propulsion Information Agency, p. 366.

[5] Webb, L. D., Harris, R. W., and Cook, E. T., III, "Study and Literature Survey of Stress State Transducer Development," TR AFRPL-TR-69-74, March 1969, Air Force Rocket Propulsion Lab., Edwards Air Force Base, Calif.

[6] Hilzinger, J. E., "Microstructural Behavior of Filler Reinforced Elastomeric Systems," *Proceeding of 5th Meeting, Mechanical Behavior Working Group*, Vol. I, ICRPG, CPIA Publication No. 119, Nov. 1966, Interagency Chemical Rocket Propulsion Group and Chemical Propulsion Information Agency, p. 169.